Journal of the Korean Vacuum Society
Vol. 2, No. 3, September 1993, pp. 304-313

〈연구논문〉

Application and Development of Focused Ion Beams

Seung Oun Kang

Department of Physics, Kwangwoon University, Seoul 139-701, Korea
(Received July 9, 1993)

집속 이온빔의 응용 및 개발

강 승 언

광운대학교 이과대학 물리학과
(1993년 7월 9일 접수)

Abstract – Focused ion beam (FIB) technologies have been widely used in microfabrication of semiconductor devices: high resolution ion beam lithography, maskless ion implantation, micro-machining, and ion beam induced deposition. A liquid gallium ion source for the use of in FIB has been developed and tested in Korea, showing good stability, high current density, small energy spread, and low emittance or high brightness. A electrostatic einzel lens is designed and constructed to have a beam diameter of 0.1 μm after passing through the lens column under a beam voltage of 15 kV, lens voltage of 7 kV and 0.2 mm diameter of beam defining aperture placed in front of the lens. The FIB chamber has been also designed and constructed with a differential vacuum system from the lens column. It is expected that the FIB machine will have great contribution to the applications of ion beam milling, ion beam induced deposition, and failure analysis in semiconductor industry in Korea in the near future.

요　　약 – 집속 이온빔 기술은 고해상도의 이온빔 리토그라피, 마스크가 필요없는 이온주입, 그리고 Ion beam induced deposition 등 반도체 소자의 미세가공에 널리 이용되어 왔다. 좋은 안정도와 높은 전류밀도, 적은 에너지 퍼짐 그리고 낮은 에미턴스와 높은 선명도를 갖는 집속 이온빔 장비를 위한 액체 갈륨 이온원이 한국에서 개발 시험되었다. 이온빔의 전압이 15 kV, 렌즈전압이 7 kV 그리고 렌즈상단에 위치한 aperture의 직경이 0.2 mm일 때, 0.1 μm의 빔 직경으로 집속되는 정전 einzel 렌즈가 설계 조립되었고, FIB 진공 chamber는 렌즈부와의 차 등 진공시스템으로 구성되어 설계 제작되었다. FIB 장비가 조만간 한국에서 이온빔 밀링, ion beam induced deposition 그리고 잘못된 부분의 수정 등 반도체 제작공정에서의 응용에 큰 기여를 할 것이라 기대된다.

1. Introduction

There has been great interest in the Focused Ion Beam (FIB) technology during the last decade. The FIB is an appropriate tool in developing submicrometer structures necessary for high density integrated circuits in semiconductor industries. The Liquid Metal Ion Sources (LMIS), moreover, opened the possibility of FIB application to the actual manufacturing processes. The study of LMIS was initiated with an interest in an application to the rocket propulsion. It was soon realized, however, that the source had an excellent focusing property that could be utilized for a FIB system. The LMIS have a high current density, a high brightness, a low energy spread (5～20 eV) and a low emittance. These characteristics greatly reduce various aberration effects in the course of focusing, and make it possible for the ion beam to be focused in a scale down to a few tens of nanometers.

Followings are just a few out of diverse potential application areas of FIB system employing the

LMIS[1].

(1) Scanning Ion Microscopy (SIM)
(2) X-ray and Optical Mask Repair
(3) Secondary Ion Mass Spectrometry (SIMS)
(4) Ion Beam Lithography
(5) Maskless Implantation Doping of Semiconductor
(6) Failure Analysis and Micromachining
(7) Ion Beam Induced Deposition

These application areas commonly require ion beams of finely focused. Most of them are modification or extension of existing technologies well known to the semiconductor industry. In the present article, we review some of the applications to the SIM, ion beam induced deposition and the lithography, and current research stages in Korea.

2. Application of FIB

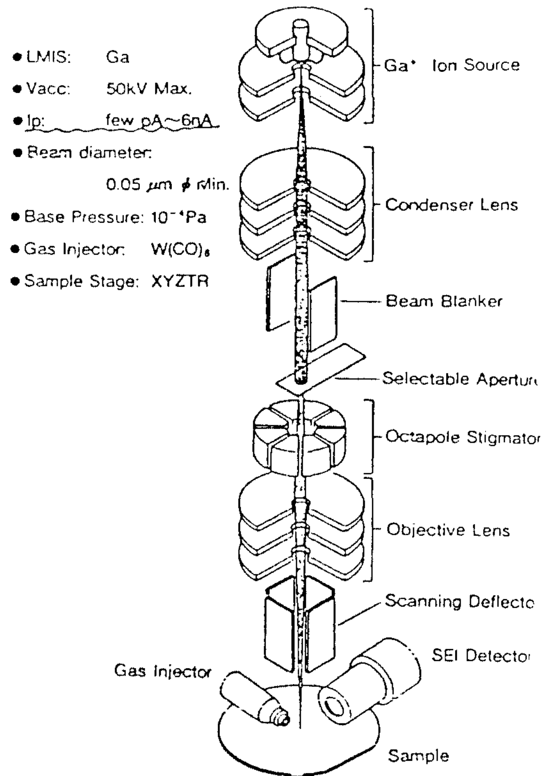

Fig. 1. Basic elements of focused ion beam system.

Fig. 1 illustates the basic elements of a focused ion beam system. The ion optical column consist of a LMIS, two electrostatic focusing einzel lens (condenser lens and objective lens), beam blanker, variable aperture, octapole stigmator, scanning deflector, and a sample stage. Ions emitted from the LMIS are focused onto the target as a submicron spot size. For the application to lithography, etching, milling and mask repairs, Ga ions are commonly used. For the application to maskless implantation or doping, ions, such as those of Si, B, and As, are used. Since the material compounds involving these atoms have generally high melting points, alloyes of them are employed to bring down the melting point. The optical column for these ions, consequently, requires addition of a mass filter in order to seperate out the desired ions. The beam can be raster scanned at video rates to produce scanning ion image or deflected in a programed pattern under computer control for lithography, mask repair, failure analysis etc. The key element of the FIB system is the LMIS, which will be described at section 3.

2.1. Scanning Ion Microscopy (SIM)

A scanned focused ion beam can produce an image of a sample in a manner analogous to a scanning electron microscopy (SEM). The ion is raster scanned over the sample. Low energy secondary electron are ejected from the sample surface in the region struck by the ion beam. The secondary electron yield depends on the surface topography, work function, chemical composition, and crystal orientation of the sample. The secondary electron are typically detected with either a channeltron electron multiplier or a scintillator to produce an analog signal whose amplitude is propotional to the secondary electron yield. A example of a scanning ion image (SIM) is shown in Fig. 2[2].

2.2. Ion Beam Induced Deposition

A local gas ambient in the millitorr range is created on the surface around the point of ion incidence. The incident ions break up the gas molecules that are adsorbed on the surface. The gases consist of organometallic or metal halide. Deposits of W, Au, Al, Cr, and Pt can be made. Often these depo-

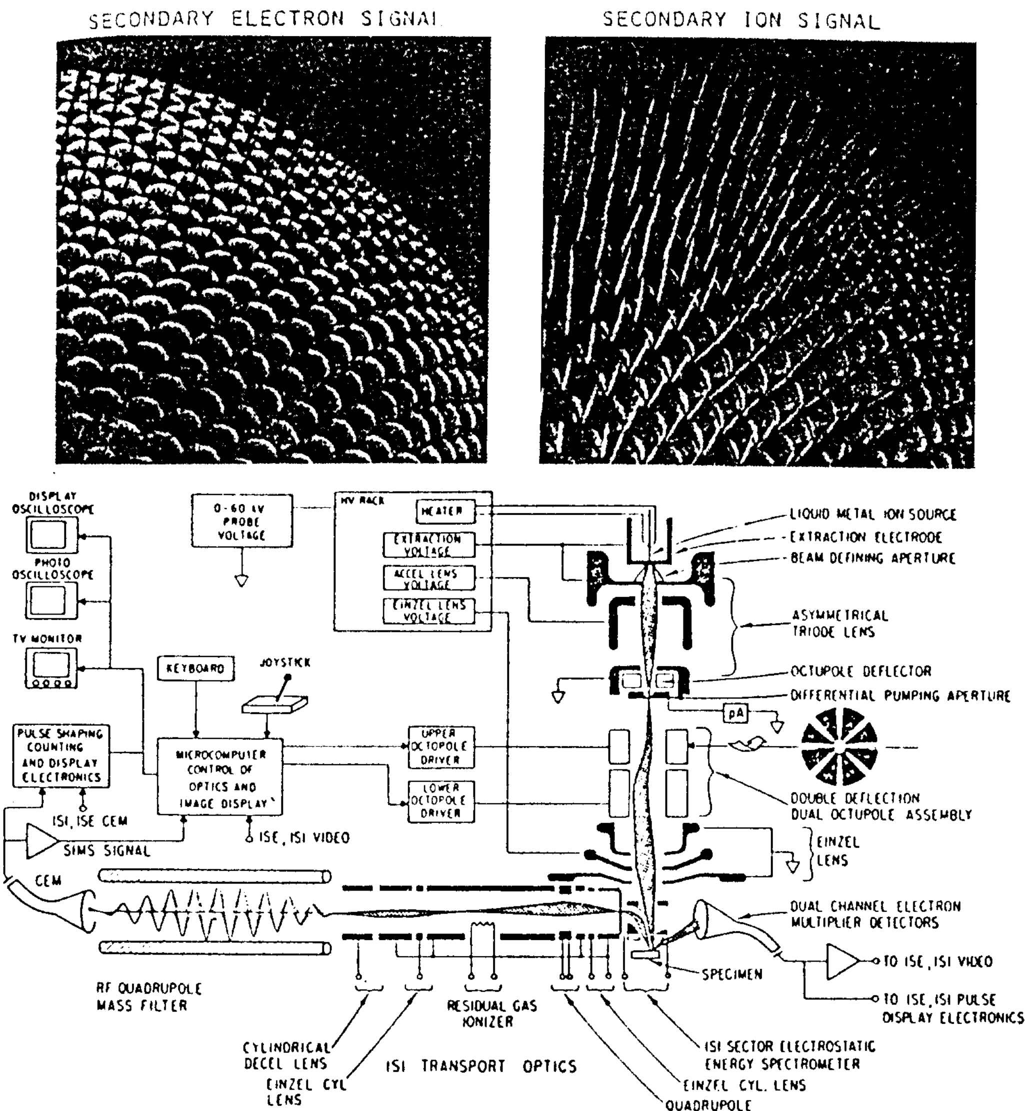

Fig. 2. Scanning ion image and SIM.

sits have high concentration of impurities, and sometimes oxygen particulaly carbon if organometallics are used.

2.3. FIB Lithography

The lithography technology using FIB have been developed by the group of J. Melngailis in MIT and S. Namba in Osaka University. Recently they have succeeded in achieving the line width of submicron. The LMIS with a good stability is essential in FIB lithography. The focused ion beam has a submicron beam diameter, however chromatic aberration resulted from ion beam energy spread sets a lower limit of beam diameter. Recently gas field ion source (GFIS) has been currently investigated by several researchers. It is known that the GFIS have extremely high brightness, small beam emitting angle less than 10°, and very small energy spread of less than 1 eV. The focusing column, beam control electronics, and substrate stage are also important factors in achieving high resolution FIB lithography. The sensitivity of resist versus ion

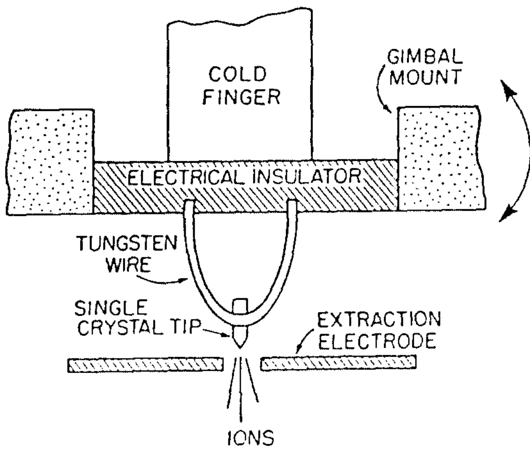

Fig. 3. Schematic of the gas field ion source.

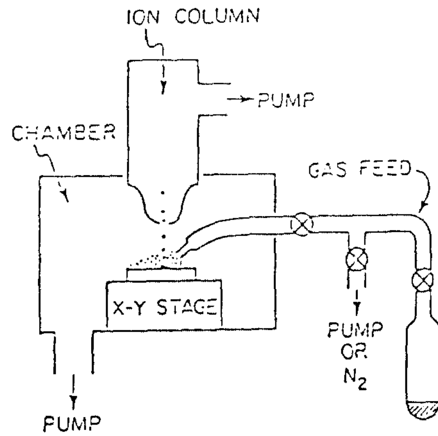

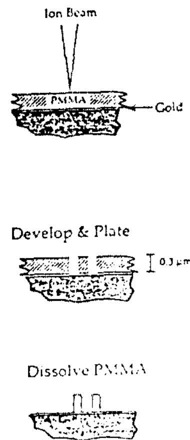

Fig. 4. Focused ion beam exposure of PMMA and electroplating of features used to fabricate x-ray lithography masks.

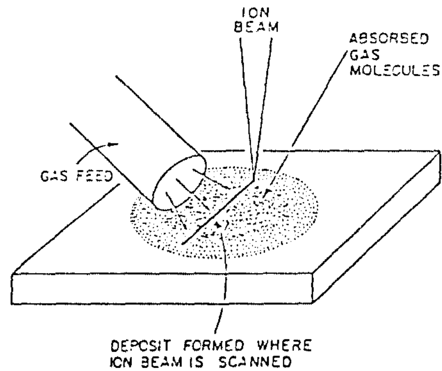

Fig. 5. Schematic of the FIB induced deposition (a) and the deposition area shown schematically close-up (b).

beam energy should be improved. Fig. 3 shows the schematic of gas field ion source. The result of FIB lithography[3] is shown in Fig. 4.

Schematic of FIB induced deposition system is shown in Fig. 5(a). A FIB column is mounted a vacuum chamber so that ion beam is focused on a sample. The system configuration looks like a scanning electron microscopy or an electron beam lithography machine. This creates a local gas ambient on the range of 1 to 10 mtorr over an area of the surface which is usually larger than the field scanned by the ion beam (Fig. 5(b)). The vacuum chamber is pumped so that the pressure away from the gas feed is typically in 10^{-6} torr range. Usually the ion column is pumped differentially[4].

For the repair of integrated circuits the films need to be conducting. Frequently carbon or tungsten has been used. A typical sequence to connect two conductors is shown in Fig. 6. Vias are milled first with the FIB by scanning small rectangles over the passivation until the metal is exposed, as shown in the middle. Imaging in the SIM mode can be used for the end point detection since the secondary electron yield of the metal is usually higher than that of the passivating oxide. Finally (bottom) a metal connector is made by focused ion beam induced deposition. The properties of some of the films by the ion induced process are summarized in Table 1.

3. FIB System Development in Korea

3.1. Liquid Gallium Ion Sources

3.1.1. Current-voltage (I-V) and Angular Distribution Characteristics

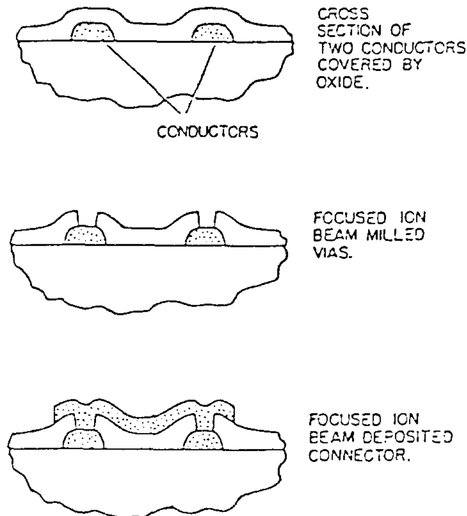

Fig. 6. Schematic of circuit repair of restructuring.

The current-voltage (I-V) characteristics and angular distributions of current density of liquid Ga ion source are investigated under various emitting tip temperatures and surface flow impedances. Fabrication of LMIS and the emitting electrode is described in detail in Ref. [5] Gallium is loaded on the region between central bottom of tungsten ribbon and needle type tungsten tip. The temperature of the emitting-tip can be controlled by adjusting the heating current IH and voltage VH. The angular distribution of emitted ion current density is investigated by measuring the current signals in each segment of collector consisted of six concentric rings forming a hemisphere[6]. The protruded tip length from central hole of heating tungsten ribbon to the tip end is maintained at 2 mm. The central hole of the extractor is 3 mm in diameter and its angle of inclination is 45° with respect to vertical axis, respectively. The spacing between the emitting tip and extractor is maintained to $d_1=1$ mm. For heating currents with $I_H=2$, 4, and 6 amps through tungsten ribbon, the corresponding temperatures of Ga loaded region are measured to be

Table 1. Ion induced deposition characteristics

Gas (Reference)	Ion energy	Yield (atoms/ion)	Deposit composition	Resistivity (μΩcm)
Styrene[a]	Ga^+ 20 keV	3.6	C : O(65 : 30)	
WF_6[b,i]	Ar^+ 500 eV and 2 keV		W : F : C(93.3 : 4.4 : 2.3)	15
$W(CO)_6$[c]	Ga^+ 25 keV	2	W : C : Ga : O (75 : 10 : 10 : 5)	150~225
$W(CO)_6$[d] (40℃)	Ga/In/Sn 16 keV		W : C : O(50 : 40 : 10)	100
$C_7H_7F_6O_2Au$[e]	Ga^+ 40 keV(room T)	3~8	Au : C : Ga(50 : 35 : 15)	500~1500 (Bulk Au=2.44)
$C_7H_7F_6O_2Au$[f]	Ga^+ 40 keV at 120℃	3	Au : C : Ga(80 : 10 : 10)	3~10
$C_9H_{17}Pt$[g]	Ga^+ 35 keV	0.2~30	Pt : C : Ga : O (45 : 24 : 28 : 3) (24 : 55 : 19 : 2)	70~700 (Bulk Pt=10.4)
$(CH_3)_3NAlH_3$[j]	Ga^+ 20 keV	4~6	Al : Ga : C : N	900 μΩcm
$Si(OCH_3)_4+O_2$[h]	Si^{++} 60 keV	1 (molecule/ion)	SiO_x (no carbon)	2.5 (MΩcm)

[a]L. R. Harriott and J. Vasile, *J. Vac. Sci. Technol.* **36**, 1037 (1988); [b]Z. Xu, T. Kosugi, K. Gamo and S. Namba, *J. Vac. Sci. Technol.* **B7**, 1959 (1989); [c]D. K. Stewart, L. A. Stern and J. C. Morgan, SPIE (1989); [d]Y. Madokoro, T. Ohnishi and T. Ishitani, Riken Conf. Mar. 1989; [e]P. G. Blauner, J. S. Ro, Y. Butt and J. Melngailis, *J. Vac. Sci. Technol.* **B7**, 609 (1989); [f]P. G. Blauner, Y. Butt, J. S. Ro, C. V. Thompson and J. Melngailis, *J. Vac. Sci. Technol.* **B7**, 1816 (1989); [g]T. Tao, J. Melngailis, Z. Xue and H. D. Kaesz, EIPB 1990 and to be published *J. Vac. Sci. Technol.* (1990); [h]H. Komano, Y. Ogawa and T. Takigawa, *Japn. J. Appl. Phys.* **28**, 2372 (1989); [i]K. Gamo and S. Namba, Proc. 1989 Intern. Symp. on MicroProcess Conf. p. 293; [j]M. E. Gross, L. R. Harriott and R. L. Opila, *J. Appl. Phys.* **68**, 4820 (1990).

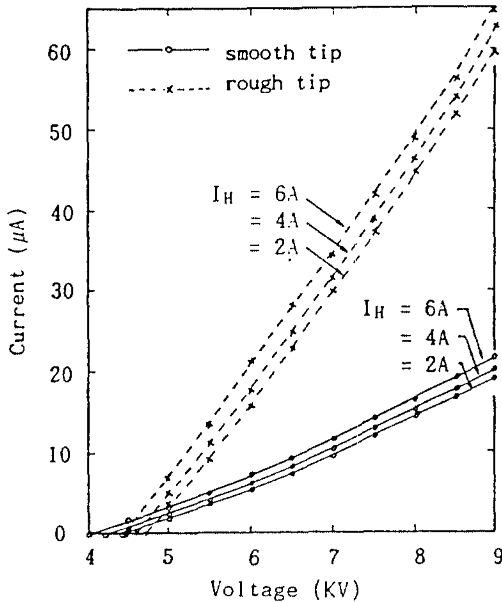

Fig. 7. I-V charateristic curves: The dotted and solid lines are represented by $d_1=1$ mm with rough surface and with smooth surface, respectively. The heating current are varied as $I_H=2$, 4 and 6 amps.

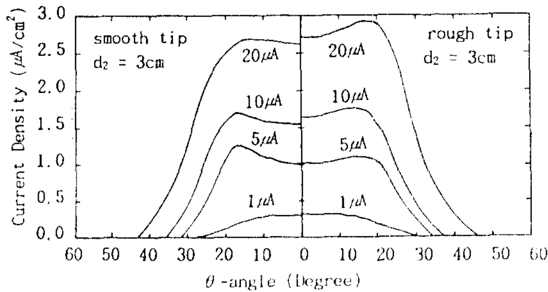

Fig. 8. Angular distribution of current density under fixed location of collector cups $d_2=3$ cm: The left and right hand sides of this figure are represented by $d_1=1$ mm with smooth surface and rough surface, repectively.

335 K, 391 K and 530 K, respectively. Fig. 7 shows the I-V characteristics for $d_2=3$ cm, where d_2 is interdistance between emitting tip end and central segment of collector cups. Solid and dotted lines in this figure are corresponded to smooth and rough tip, respectively. The slope of dI/dV is shown to be about 3 μA/kV for a smooth surface, while 12 μA/kV for a rough surface. The emitting current is also shown to increase as the heating current is increased but the slope (dI/dV) remains the same. Fig. 8 shows the angular distribution of the current densities for the tip with a smooth surface and for the tip with a rough surface, under fixed location $d_2=3$ cm of collector cups. For further locations of d_2, the similar angular distributions of current densities are shown generally. From this figure we see that the angular distributions of current density for both cases of flow impedances are remarkably similar within the experimental error for the same amount of emission current under fixed locations of the collector cups. These results mean that the surface profiles of ion emitted liquid metal sources have identical shape for the same amount of the emission current. This implies that the amount of the ion emission current is determined by the surface profiles of the liquid metal film [7].

3.1.2. Energy Deficit and Energy Spread Characteristics

Energy distribution, energy deficit and its spread of ions emitted from a liquid gallium ion source have been investigated by a gridded retarding potential analyzer with 0.2 volt resolution in which nickel mesh spacing is 33.8 μm under the source temperature of 335 K. Fig. 9(a) shows that the energy distributions of a liquid gallium ion source are Maxwellian for emission currents from 5 μA up to 40 μA. Fig. 9(b) shows that the energy spread (FWHM) is increased with a power of $I^{0.8}$ from 4.3 eV up to 45 eV as emission current is increased from 1 μA up to 50 μA. This energy spread results from space charge interactions among ions. Fig. 9(c) shows that the peak energy deficit is ranged from −8 eV up to 4 eV as the emission current is increased from 1 μA up to 50 μA. From this energy deficit measurement, it's determined that the liquid gallium ions are singly charged Ga^+ monomer ions and generated mainly by field evaporation mechanism in this low source temperature. At higher source temperature of 700 K, the cluster Ga_n^+ ($n=2$, 3) ion beam is believed to be generated by field ionization mechanism from the energy deficit measurements. At this case the energy deficit is ranged from −13 eV up to 70 eV as emission current is

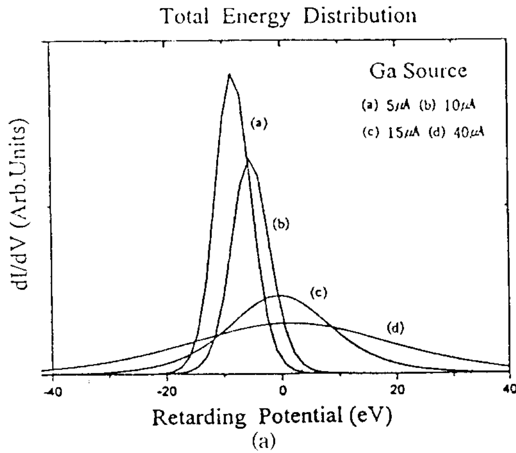

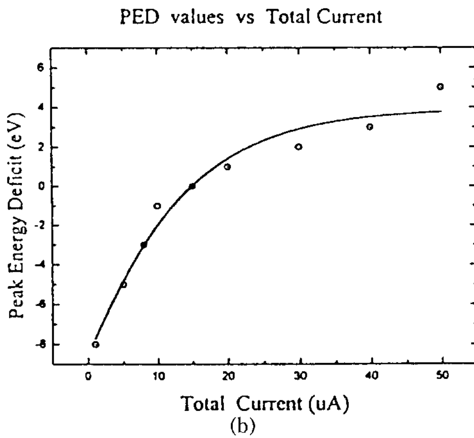

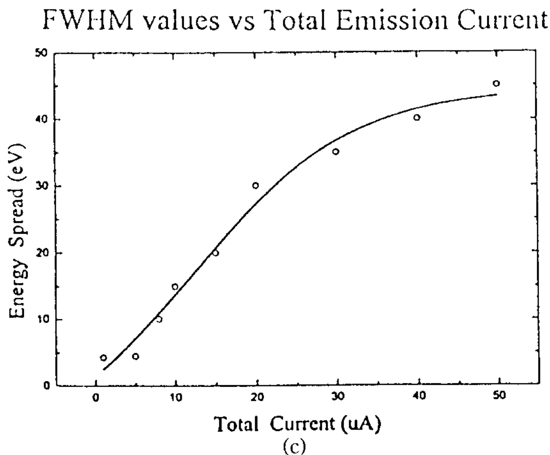

Fig. 9. Energy distribution of liquid gallium ion source (a), Energy spread (b), Peak energy deficit (c): The heater current is fixed to $I_H=2$ amps.

increased from 5 μA up to 50 μA.

3.1.3. Figure of Merit for FIB

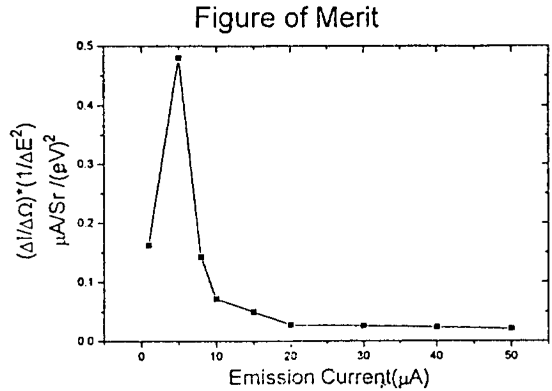

Fig. 10. Figure of merit versus emission current.

The optimum range of total ion current for a liquid gallium ion source for use as a focused ion beam (FIB) is determined from a figure calculated from the angular intensity $dI/d\Omega$ and the energy spread ΔE of the emitted ions. In general, when the ion source in a FIB instrument is operated to give a probe current less than several nA, the diameter of the FIB is largely determined by the chromatic aberration resulted from the energy spread. The current density of this chromatic aberration disk is given by $J=(E^2/C_c^2)\ (\Delta I/\Delta\Omega)/(\Delta E)^2$, where E and C_c are the energy of the ion beam and the coefficient of chromatic aberration, respectively. The figure of merit (FM) is defined as $FM=(\Delta I/\Delta\Omega)/(\Delta E)^2$. The optimal emission current for FIB is obtained by maximizing the FM because at which the smallest chromatic aberration disk is achieved. Fig. 10 shows the plot of FM versus emission current, in which FM has the maximum value of 0.48 μA/sr/(eV)^2 at the optimal emission current of 5 μA. With this optimal emission current, the focused ion beam passed through einzel lens is expected to have a beam diameter of 0.1 μm under beam voltage 15 kV and 0.2 mm diameter of beam defining aperture placed in front of lens.

3.1.4. Emittance Measurements

The root mean square (rms) emittance for an axisymmetric and nonrotating liquid gallium ion beam with a Maxwellian transverse distribution is investigated by using a slit-hole type emittance meter and a radiachromic detector film. The emittance meter is consisted of 5 slits whose spacing is maintained at 130 μm. The axial interdistance between

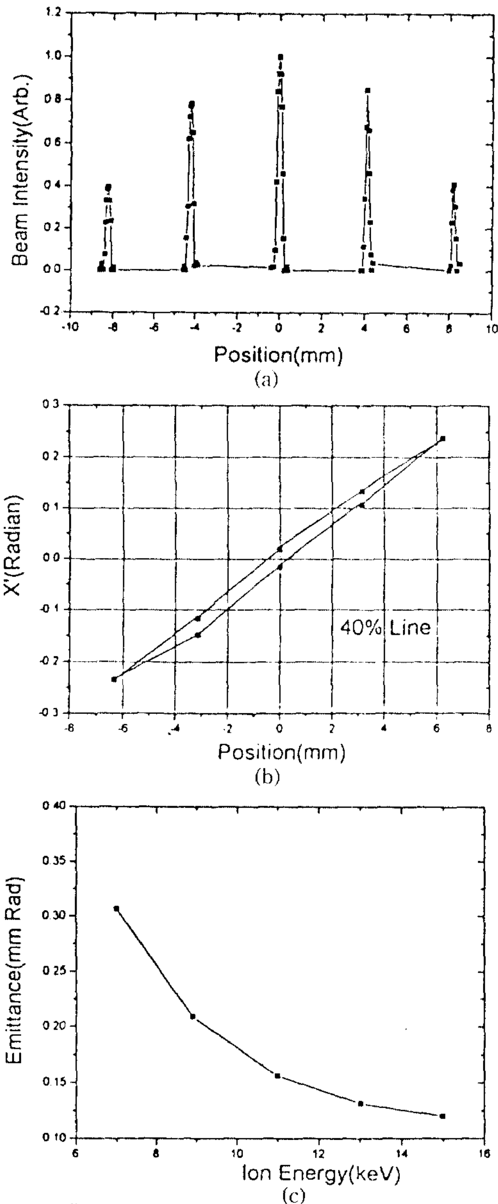

Fig. 11. Total intensity profiles versus slit position (a), Emittance diagram fo 40% line of peak intensity (b), Emittance versus beam energy (c).

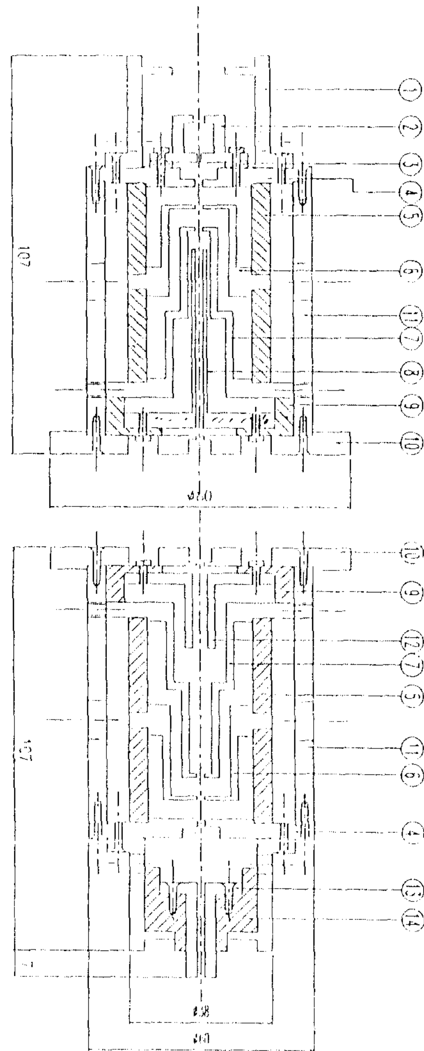

Fig. 12. Design of electrostatic einzel lens.

the spatial plane (slit plane) and angular plane (detector film) is kept at 8 mm. In this experiment, the vacuum is maintained at 1.0×10^{-5} torr and the emission current is kept at 10 μA. The rms emittance[8] is defined by $\varepsilon_{rms}=4(\langle x^2\rangle\langle x'^2\rangle-\langle xx'\rangle^2)^{1/2}$, where x and $x'=dx/dz$ denote slit position and gradient of particle trajectory, respectively. The brackets (< >) denote values averaged over the phase space. Fig. 11(a) shows the total intensity profiles versus the slit positions. From this figure, we can see that the intensity distributions and the rms widths for given slit positions reveal Gaussian profiles. Also the peak intensity profiles versus the slit positions are shown to be Gaussian. Fig. 11(b) shows the emittance diagram for 40% line of peak intensity. From this figure, the liquid gallium ion beam is shown to be linearly focused as a whole before it enters the einzel lenses. The plot of emittance versus beam energy is drawn in Fig. 11(c). The emittance is decreased from 0.30 mm-rad to

0.12 mm-rad as the beam energy is increased from 7 keV up to 15 keV. The mean transverse beam temperature is measured to be approximately $T_\perp = 4$ eV.

3.2. Electrostatic Lens and FIB Chamber

The electrostatic einzel lens system is designed and developed to focus a liquid gallium ion beam. Fig. 12 shows the design of electrostatic einzel lenses to focus a liquis gallium ion beam. The single lens has 107 mm in length and the stainless steel is used as electrodes. The lens system are consisted of a Faraday cup, a condenser lens, a blanker, a octopole stigmator, object lens, and a deflector. The focused ion beam passed through the single einzel lens is expected to have a beam diameter of 0.1 μm under beam voltage 15 kV, lens voltage 7 kV, and 0.2 mm diameter of beam defining aperture placed in front of lens. Fig. 13 shows the schematic of the FIB system. The FIB chambers are consisted of 3 parts; source chamber, lens chamber and specimen chamber, respectively. The whole length of this chamber is 720 mm. The outer diameter of source chamber and the lens chamber is 160 mm and 5 mm in thickness. The ion pump has been used to evacuate the source chamber down to 1.0×10^{-8} torr through differential pumping method. The source chamber is made of stainless steel and 213 mm in length. The variable aperture is located in the lens chamber. The lens chamber is made of stainless steel and 207 mm in length. The lens high voltage is applied through high voltage input placed at the lens chamber. The specimen chamber is made of stainless steel. It has 330 mm in length and 470 mm in diameter, respectively. The motorized slides with *x-y* translation and tilting has been set in this chamber. Specimen chamber is evacuated down to 1.0×10^{-6} torr with roughing and turbomolecular pumps. The lens chamber and specimen chamber are designed to be evacuated by differential pumping and isolated by a column isolation valve when ion beam is not emitted from the source.

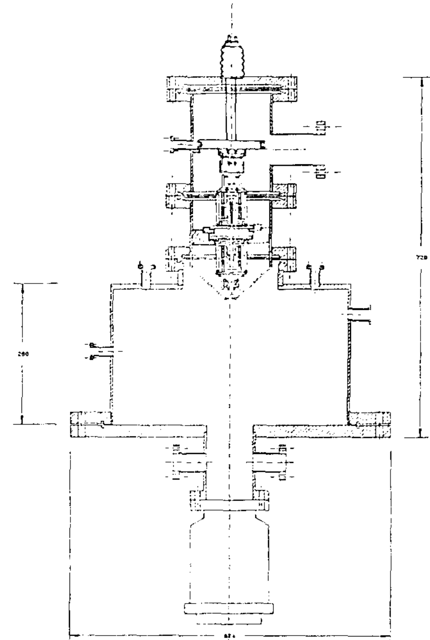

Fig. 13. Schematic FIB system.

4. Conclusion

The liquid gallium ion source with good stability has been developed for use in FIB. The I-V characteristics and angular distributions of the current density of liquid gallium ion source has been performed under various emitting temperatures and surface flow impedances. For the same amount of the emitting current under various tip surface conditions and applied tip voltages, the surface profiles of the ion emitted liquid metal film are taken to be identical shape. The energy distribution, energy deficit and its spread of ions emitted from a liquid gallium ion source have been investigated by a gridded retarding potential analyzer with 0.2 volt resolution in which nickel mesh spacing is 33.8 μm under the source temperature of 335 K. The energy spread (FWHM) is increased with a power of $I^{0.8}$ from 4.3 eV up to 45 eV as the emission current is increased from 1 μA up to 50 μA. This energy spread is resulted from space charge interactions among ions. Energy deficit is shown to be ranged from −8 eV up to 4 eV as the emission current is increased from 1 μA up to 50 μA. From this energy deficit measurement, the liquid gallium ions are singly charged Ga^+ monomer ions and generated mainly by field evaporation mechanism. The optimal emission current for FIB is obtained by

maximizing the figure of merit (FM). FM has the maximum value of 0.48 μA/sr/(eV)^2 at the optimal emission current of 5 μA. With this optimal emission current, the focused ion beam passed through einzel lens is expected to have a beam diameter of 0.1 μm under beam voltage 15 kV and 0.2 mm diameter of beam defining aperture placed in front of lens. The root mean square (rms) emittance for an axisymmetric and nonrotating liquid gallium ion beam with a intensity. The liquid gallium ion beam is shown to be linearly focused as a whole before it enters the einzel lenses. The emittance is decreased from 0.30 mm-rad to 0.12 mm-rad as beam energy is increased from 7 keV up to 15 keV. The mean transverse beam temperature is measured to be approximately $T_{\perp}=4$ eV. The electrostatic einzel lens system is designed and developed to focus a liquid gallium ion beam. The structures of lens system are consisted of Faraday cup, condenser lens, blanker, octapole stigmator, object lens, and deflector. The FIB chambers are consisted of 3 parts; source chamber; lens chamber and specimen chamber, respectively. The ion pump has been used to evacuate the source chamber down to 1.0×10^{-8} torr through differential pumping method. The motorized slides with *x-y* translation and tilting has been set in the specimen chamber. The specimen chamber is evacuated down to 1.0×10^{-6} torr with roughing and turbomolecular pumps. The lens chamber and specimen chamber are designed to be evacuated by differential pumping and isolated by a column isolation valve when the ion beam is not emitted from the source.

References

1. A. Wagner, Proceeding of 11th conferece on electron and ion beam sciences and thechnology, P9, 167 (1983).
2. Levi Setti, Research Report, Scanning Ion Microprobe & FIB Applications (1984).
3. J. Melngailis, Nuclear Instr. and method in Physics Research B, to be Published.
4. X. Xu, A. D. Ratta, J. Sosonkina and J. Melngailis, *J. Vac. Sci. Technology* **B10**, 2695 (1992).
5. S. O. Kang, G. S. Cho and T. W. Kim, *Korean Appl. Phys.* **4**, 246 (1991).
6. (a) G. S. Cho, E. H. Choi and S. O. Kang, *Korean Appl. Phys.* **5**, 611 (1992); (b) G. S. Cho, E. H. Choi, Y. H. Seo, T. W. Kim and S. O. Kang, *J. Appl. Phys.* (will Be Published August (1993)).
7. (a) G. S. Cho, E. H. Choi and S. O. Kang, *Korean Appl. Phys.* **5**, 616 (1992); (b) G. S. Cho, Y. H. Seo and S. O. Kang, *J. Appl. Phys.* **72**, 5892 (1992).
8. F. J. Sacherer, *IEEE Trans. Nucl. Sci.* **NS-18**, 1105 (1971).